Atomistic simulations of a solid/liquid interface: a combined force field and first principles approach to the structure and dynamics of acetonitrile near an anatase surface

2008 J. Phys.: Condens. Matter 20 064206

(http://iopscience.iop.org/0953-8984/20/6/064206)

J. Phys.: Condens. Matter **20** (2008) 064206 (8pp) doi:10.1088/0953-8984/20/6/064206

Atomistic simulations of a solid/liquid interface: a combined force field and first principles approach to the structure and dynamics of acetonitrile near an anatase surface

Florian Schiffmann, Jürg Hutter and Joost VandeVondele

Physical Chemistry Institute, University of Zurich, Winterthurerstrasse 190, CH-8057 Zurich, Switzerland

E-mail: Joost.VandeVondele@pci.uzh.ch

Received 20 August 2007, in final form 2 November 2007
Published 24 January 2008
Online at stacks.iop.org/JPhysCM/20/064206

Abstract

The acetonitrile/anatase(101) interface can be considered a prototypical interface between an oxide and a polar aprotic liquid, and is common in dye sensitized solar cells. Using first principles molecular dynamics simulations of a slab of TiO_2 in contact with neat acetonitrile (MeCN), the liquid structure near this interface has been characterized. Furthermore, in order to investigate properties that require extensive sampling, a classical force field to describe the MeCN/TiO_2 interaction has been optimized, and we show that this force field accurately describes the structure near the interface. We find a surprisingly strong interaction of MeCN with TiO_2, which leads to an ordered first MeCN layer displaying a significantly enhanced molecular dipole. The strong dipolar interactions between solvent molecules lead to pronounced layering further away from the interface, each successive layer having an alternate orientation of the molecular dipoles. At least seven distinct solvent layers (approximately 12 Å) can be discerned in the orientational distribution function. The observed structure also strongly suppresses diffusion parallel to the interface in the first nanometer of the liquid. These results show that the properties of the liquid near the interface differ from those in the bulk, which suggests that solvation near the interface will be distinctly different from solvation in the bulk.

1. Introduction

Dye sensitized solar cells (DSSCs) are photovoltaic devices that promise to become technically and economically credible alternatives to the more standard silicon based cells [1–3]. These devices function by virtue of light induced electron transfer at the interface between a semiconductor, a dye and an electrolyte. So far, the best performing dyes found are transition metal complexes, while a typical electrolyte used in these cells is based on an organic solvent such as acetonitrile (MeCN), and the I^-/I_3^- redox couple. A real breakthrough in the field of DSSCs was made in 1991 by Grätzel and co-workers [1, 2], when anatase nanoparticles were introduced to replace bulk semiconductors. The large surface area of this material led to a very significant increase in the incident photon to currency efficiency (IPCE) of these cells. Nevertheless, despite several years of additional research into DSSCs, these cells cannot yet compete with cells based on more traditional approaches, and further insight is needed to improve and tune the properties of the interface [4].

A number of density functional theory (DFT) based studies have investigated various components of this interface [5]. For example, electronic properties of various dyes in the gas phase, in implicit solvents, or attached to small clusters of TiO_2 have been studied [6–11]. Other workers have employed a slab geometry for the semiconductor, and have investigated

electronic properties or binding affinities of model compounds and organic dyes at these surfaces [12–15]. The computational cost of describing large slabs of TiO_2 has so far prohibited the study of the larger transition metal dyes on the surface. To the best of our knowledge, none of the atomistic studies performed so far takes the solvent, or even better the electrolyte, explicitly into account. It is our goal, eventually, to study the process of electron transfer at this interface in a quantitative way, which requires an explicit model for all aspects of this interface. For example, there is a big difference in the absorption spectra and the stability of a free dye in solution and one attached to the surface [5]. Indeed, the important role of the solvent has been emphasized since Marcus's work on electron transfer [16–18]. The solvent determines not only the relative stability of the various charged and neutral species, but through the solvent reorganization energy also the rate of electron transfer. In some of our previous work, we have shown that DFT based simulations using an atomistic representation of the solvent can capture these effects rather well, allowing for quantitative agreement with experiment for differences in redox potentials and solvent reorganization energies, even for large systems such as proteins [19–22]. In this work, we wish to focus on the solid/liquid interface that is most relevant in DSSCs, namely the anatase(101)/acetonitrile interface. Indeed, anatase nanoparticles expose several crystal surfaces to the solvent, but anatase(101) is the dominant structure. Previous work on describing solid/liquid interfaces with DFT has mainly focused on metal–water interfaces, given their importance in fuel-cell catalysis [23–25]. However, water, with its strong hydrogen bonding, is a rather particular liquid, quite different from the organic solvents typically encountered in DSSCs, while metal/substrate interactions are quite distinct from semiconductor/substrate interactions.

The remainder of this article is organized as follows. In section 2 we discuss our computational set-up, and the CP2K/Quickstep simulation package [26]. The simulation of interfaces is computationally very demanding, but, as we will show below, the efficiency of CP2K allows us to perform molecular dynamics simulations, ≈10 000 Born–Oppenheimer molecular dynamics (MD) steps, of more than 600 atoms and a total of 2800 electronic states. In section 3 we derive and validate a classical force field (FF) to describe the TiO_2/MeCN interface. This FF allows us to obtain improved statistical accuracy for properties that require long sampling to reach convergence. In section 4, we discuss the structure of the liquid at the interface. Anticipating our results, we find pronounced layering of the solvent up to about 12 Å away from the interface, and a much increased molecular dipole of the solvent molecules in the first layer. Dynamic properties of the solvent are discussed in section 5, where diffusion parallel to the surface is studied. We compute the position dependent diffusion constant of the liquid, and find that diffusion is strongly suppressed in the interfacial region. Finally, in section 6, we summarize our findings and discuss the possible implications for solvation near interfaces, and for DSSC in particular.

2. Computational set-up

All molecular dynamics simulations reported in this work have been performed using the CP2K simulation package [26]. A time step of 0.5 fs and the microcanonical ensemble (NVE) have been employed for both *ab initio* and classical MD simulations. Force field based molecular dynamics simulations are based on smooth particle mesh Ewald and neighborlist techniques, which are common in bio-molecular simulation packages and lead to efficient and linear scaling implementations. The derivation of the FF used, is discussed in detail in the following section.

The density functional implementation in CP2K (Quickstep) has recently been reviewed in detail in [27], and is based on the hybrid Gaussian plane wave (GPW) scheme [28]. In this scheme, an efficient and linear scaling algorithm for the calculation of the Kohn–Sham matrix is obtained through a dual representation of the electron density. Whereas the wavefunctions are always represented using Gaussians, the electron density can be represented either in Gaussians (the primary basis) or in plane waves (the auxiliary basis). The transformation of representation between these basis sets can be performed efficiently [27]. The advantage of the Gaussian basis set is its localized nature, which leads to sparse matrix representations of the required operators, and the fact that only a small number of basis functions (relative to e.g. a plane wave basis set) is required to represent the wavefunctions accurately. The advantage of using an auxiliary plane wave basis set for the density is that fast Fourier techniques can be employed to compute the electrostatic (Hartree) energy, avoiding the traditional bottleneck of Gaussian based DFT codes. Wavefunction optimization is performed using the orbital transformation minimizer, which guarantees convergence and avoids diagonalization of the Hamiltonian matrix [29]. The Perdew–Burke–Ernzerhof (PBE) functional [30] and Goedecker–Teter–Hutter (GTH) pseudopotentials [31–33] have been employed for all DFT calculations. A 280 Ryd plane wave density cut-off has been applied. Carbon, hydrogen and nitrogen of the MeCN molecules were described using a standard triple-ζ basis with two sets of polarization functions (TZV2P). In previous work, we obtained satisfactory results for structure and dynamics of liquid acetonitrile with this basis set [21]. For the oxide, a recently developed procedure to derive molecularly optimized basis sets [34] has been employed to derive basis sets for titanium and oxygen. Using five primitives, basis sets of double-ζ quality have been optimized on small Ti–O compounds. An important advantage of these molecularly optimized basis sets is that they can be diffuse, even in the condensed phase, without introducing near linear dependencies in the basis [34]. Near linear dependencies can cause instabilities in the SCF procedure, a problem encountered with more traditional split valence basis sets.

In order to assess the quality of our computational set-up, we have compared the optimized geometry of a slab of TiO_2 containing 288 atoms in three layers between CP2K and CPMD [36]. The unit cell was 15.13 Å × 20.45 Å × 22.00 Å, including 11.5 Å of vacuum to separate the slabs. Since CPMD and CP2K can use exactly the same functional,

Table 1. Computed bond lengths and bond expansions for the relaxed surface of anatase(101). Results for the bond expansion are compared to the calculations in [35]. The two non-equivalent bond lengths in the bulk are 2.002 and 1.942 Å. The labels of the atoms refer to the labels in figure 3 of [35].

	Length (Å)	Bond expansion	Reference [35]
Ti1–O1	1.84	−8.19%	−8.60%
Ti1–O2	1.98	2.16%	2.00%
Ti1–O3	2.05	2.40%	3.30%
Ti1–O4	1.79	−7.83%	−8.40%
Ti2–O1	1.85	−4.94%	−5.00%
Ti2–O2	2.01	0.20%	0.30%
Ti2–O3	1.93	−0.46%	−0.30%
Ti2–O4	2.06	3.05%	5.10%
Ti2–O5	2.15	10.92%	8.70%
Ti3–O4	2.09	7.72%	5.20%
Ti3–O5	1.96	−2.10%	−1.20%
Ti3–O6	1.94	0.00%	0.00%

pseudopotentials, and geometries, this is a good test for the quality of the basis set. A 150 Ryd plane wave cut-off for the wavefunctions has been employed with CPMD. A comparison of both optimized structures showed only differences smaller then 10^{-3} Å. DFT studies by Lazzeri *et al* [35] of different surface geometries provide a reference to judge the effect of slab size, in particular thickness (z direction) and the use of k-points. Selloni and co-workers have used two low symmetry k-points, and up to six layers of TiO_2. k-points are currently not available in CP2K, and instead larger unit cells have to be employed. For the simulations of the interface, this is not too problematic, as small unit cells would introduce a severe artificial periodicity for the liquid. As shown in table 1, the surface relaxations computed for anatase(101) in this work are in good agreement with the reference values from [35]. Similar results have been obtained for anatase(100) (not shown). The main difference in bond distances is for bonds away from the surface, which is due to the fact that the slabs used in our set-up contain just three layers.

3. Derivation and validation of the force fields

The parameters of the FF consist of three parts: (1) for the semiconductor; (2) for the MeCN liquid; (3) for the interaction between the semiconductor and MeCN molecules.

Parameters for the semiconductor and for the liquid are available in the literature; parameters for the interaction between the two are derived in this work. The TiO_2 slab is described using point charges and a Buckingham potential as parameterized by Bandura and Kubicki [15]. We employ the same bulk potential for the bulk and the surface atoms. We have verified that this potential, originally tested on rutile, led to a stable structure for anatase, with reasonable agreement to the DFT structure. For the three layer slab of anatase(101) described above the main difference between DFT and FF is a displacement of the atoms orthogonal to the surface, increasing its total thickness by about 0.3 Å. The structure exposed to the liquid has a better accuracy. Along the [101] axis atoms match within less than 0.01 Å, while displacements along the [010] vector are at most 0.05 Å.

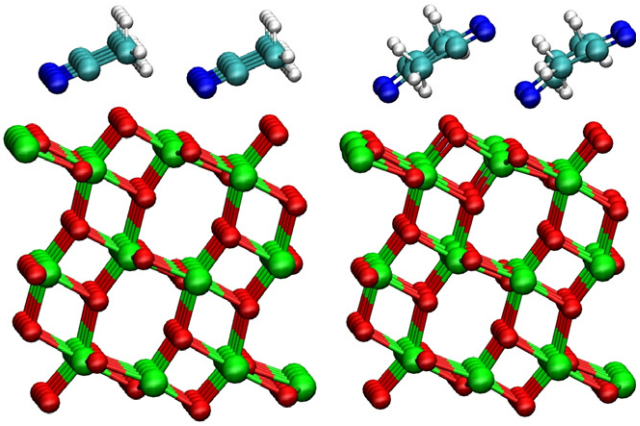

Figure 1. Shown are the optimized geometries of a monolayer of acetonitrile on a three layer anatase(101) slab. The left panel shows the parallel configuration, while the right panel shows the antiparallel configuration. The parallel configuration is the lowest energy structure. However, the antiparallel configuration is only 0.3 kcal mol^{-1} per molecule higher in energy. All atoms shown belong to the unit cell used; the three layer slab is fully optimized. (This figure is in colour only in the electronic version)

The MeCN–MeCN interactions are described using a potential based on point charges, and van der Waals interactions, while the molecular geometry is described using harmonic potentials for bonds and bends. The FF has been derived in [37] and has been shown to reproduce the structure of liquid MeCN as obtained with first principles simulations in [19].

The FF for the TiO_2/MeCN interactions is derived here. The electrostatic interaction is through the point charges mentioned previously, and parameters for a Lennard-Jones potential are optimized matching binding energies and forces along a molecular dynamics trajectory as obtained from DFT calculations. To describe the interactions of MeCN with anatase a Lennard-Jones (LJ) potential is employed. Force matching was used to optimize the parameters of the LJ potential, trying at the same time to reproduce the binding energies for a set of configurations and the forces along a DFT trajectory. Three distinct binding geometries have been used to obtain reference binding energies on a three layer slab with a 15.13 Å × 10.23 Å × 25.00 Å unit cell. One is a configuration of a single molecule interacting with the surface; in the other two cases a monolayer covered surface is used. We find that a single molecule binds with the carbonitrile group pointing towards the surface, i.e. with the negatively charged nitrogen towards the positively charged titanium. As shown in table 2, the binding energy of this configuration is relatively large (14.24 kcal mol^{-1}). Configurations of a single molecule with the methyl group pointing towards the surface are not stable. Two different binding modes for the monolayer have been identified and are shown in figure 1: one with all molecules parallel to each other, and with an orientation as described for the single molecule, and one where the MeCN molecules alternate their orientation. As shown in table 2, these two configurations have similar binding energies, the antiparallel orientation being only slightly higher in energy.

Table 2. Binding energies of MeCN to anatase(101) in kcal mol^{-1} per molecule as obtained with DFT and FF calculations. Binding energies are either for a single molecule or for a monolayer of MeCN. In the monolayer, the molecules can be oriented in the same way (parallel, as shown in the left panel of figure 1), or alternate their orientation (antiparallel, as shown in the right panel of figure 1).

	DFT	FF
Single molecule	14.24	12.58
Monolayer parallel	4.88	6.68
Monolayer antiparallel	4.56	6.26

The binding energy per molecule is, however, significantly smaller than in the case of a single molecule binding the surface. The existence of an antiparallel layer and the smaller binding energy per molecule are due to the intermolecular interactions. In the parallel case, MeCN molecular dipoles are aligned unfavorably with respect to each other, while in the antiparallel case the molecular dipoles are oriented more favorably, but the interaction with the surface is unfavorable. Furthermore, favorable N–H interactions between molecules in different rows (with N–H distances of 2.52 and 2.80 Å) further stabilize the all-parallel structure. The all-parallel monolayer resembles to some extent the low temperature (β) phase of solid acetonitrile [38]. From these monolayer calculations we can conclude that acetonitrile matches the structure of the anatase(101) surface very well.

The reference trajectory for the forces used in the force matching procedure was a short (800 fs) first principles simulation with a three layer slab containing 216 atoms and 68 MeCN molecules, of which 24 directly interacted with a surface of the slab. The unit cell of this system is 22.69 Å × 10.23 Å × 39.00 Å. This unit cell is such that it can accommodate the antiparallel monolayer, respecting its periodicity. In order to account for the two different possible binding geometries for acetonitrile, the molecules have been arranged so that half of them pointed with the carbonitrile group towards the surface and the other half with the methyl group.

In order to obtain satisfactory results with the FF, the usual combination rules for the van der Waals parameters had to be abandoned, and instead ϵ and σ had to be defined for each pair of interactions. The parameters are provided in table 3. The particularly small value of ϵ implies that this part of the potential is nearly completely repulsive. The overall interaction energy, which is attractive, reproduces the DFT results in a satisfactory manner. For example, as shown in table 2, for a single MeCN molecule binding to the surface, we obtain a binding energy of 12.58 kcal mol^{-1} with the FF, within 2 kcal mol^{-1} of the DFT results. Whereas a single molecule is underbinding, the monolayers are overbinding by about 2 kcal mol^{-1}, but the relative stability of the parallel and antiparallel monolayer is captured correctly. These results suggest that some cooperative effect at the interface is not fully captured by the FF model. Indeed, we will show in the following section that molecules near the surface exhibit a strongly enhanced molecular dipole, which is consistent with the above results. The quality of the obtained structure

Table 3. Lennard-Jones parameters for the MeCN/anatase interactions. C^{c} is the C atom of the carbonitrile group. C^{m} is the C atom of the methyl group.

i–j	ϵ_{ij}, 10^{-3} kcal mol^{-1}	σ_{ij} (Å)
H–O	6.144	2.905
H–Ti	2.064	2.613
C^{c}–O	2.397	4.423
C^{c}–Ti	5.905	2.673
N–O	2.922	4.303
N–Ti	0.701	4.131
C^{m}–O	5.833	1.681
C^{m}–Ti	7.263	4.134

Table 4. Selected interaction distances for MeCN on anatase(101) in Å as obtained with DFT and FF calculations. For the antiparallel monolayer, the two non-equivalent molecules either point with ([a]) the carbonitrile group or ([b]) the methyl group towards the surface. C^{m} denotes the methyl carbon.

		DFT	FF
Single molecule	Ti–N	2.29	2.33
Monolayer parallel	Ti–N	2.5	2.46
Monolayer antiparallel[a]	Ti–N	2.35	2.38
Monolayer antiparallel[b]	Ti–C^{m}	4.08	4.57
Monolayer antiparallel[b]	O–H	2.37	2.25

is illustrated in table 4, where we report selected distances between atoms of the surface and of the substrate. For the strong Ti–N interaction, excellent agreement is found in all cases, and the deviation between the DFT and FF structure does not exceed 0.05 Å. For those molecules pointing with the methyl group to the surface, slightly larger deviations are found, but for these configurations the influence of the intermolecular MeCN interaction is important and these FF terms have been optimized for the neat liquid. As we will shown in the next section, the parallel orientation is dominant in an equilibrium simulation of the solid/liquid interface so that we consider the FF satisfactory.

4. Solvent structure near the interface

In this section, we investigate the structure of an MeCN liquid in contact with the anatase(101) surface. For the first principles studies, we have employed a unit cell of 22.69 Å × 10.23 Å × 39.00 Å, which contains 68 MeCN molecules and a three layer anatase slab. Both sides of the slab are in contact with the liquid; the region between the slabs is fully occupied by the liquid. This system contains more than 600 atoms, and approximately 2800 doubly occupied states are needed to describe the electronic structure. A 5 ps trajectory has been computed. At the same time, FF based trajectories have been computed as well, one for exactly the same system (5 ns), and one for a significantly larger system with a unit cell of 22.69 Å × 20.46 Å × 113 Å (5 ns). The first trajectory has been used to validate the classical model, while the larger model has been used to accurately compute properties.

Already during the relatively short DFT trajectory all sites on the TiO_2 surface are occupied with MeCN, with most MeCN pointing with the carbonitrile group towards the corresponding titanium atom. A second layer in the liquid

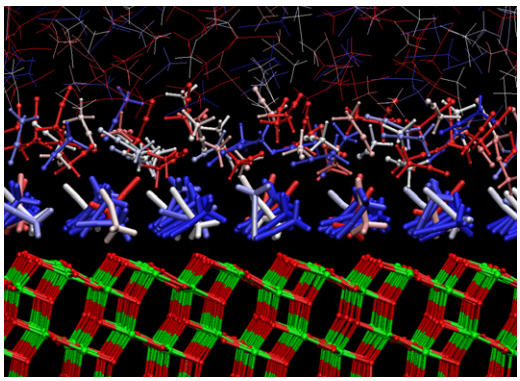

Figure 2. A snapshot from a classical simulation of the anatase(101)/acetonitrile interface. The solvent molecules are colored according to the cosine of the angle between their molecular axis and the 'ideal' axis as defined by the geometry of the all-parallel monolayer (see figure 1). The color scale goes from blue over white to red. Blue corresponds to a parallel, red to an antiparallel, and white to an orthogonal orientation. The first and second solvent layers (see text for details) are depicted using a tube and ball-and-stick representation, respectively.

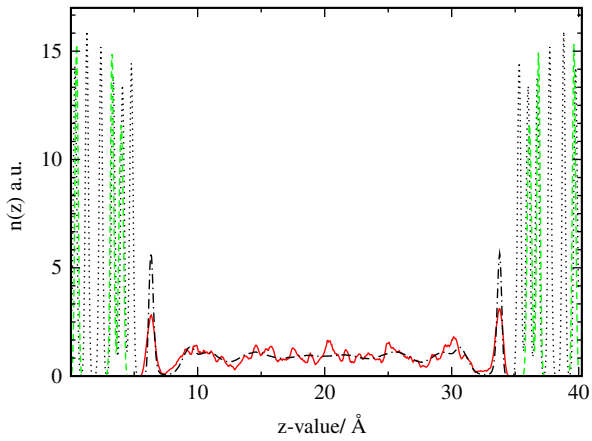

Figure 3. Shown are the density profiles of selected atom types for the DFT and FF simulations of the interface. The solid line (red) shows the nitrogen distribution as obtained from the DFT simulations. This distribution can be compared to the same distribution as obtained from the FF simulations (dash–dotted line, black). The TiO_2 slab is represented by the FF distributions of the Ti (dashed line, green) and O (dotted line, black) as obtained from FF simulations.

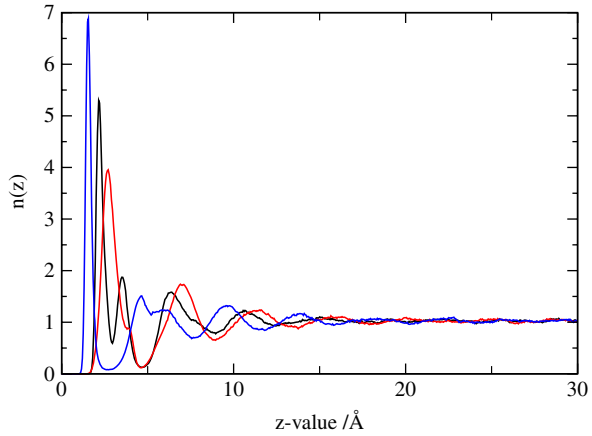

Figure 4. Shown are the density profiles of the liquid phase near the interface as obtained for the FF simulations of the interface using the large simulation cell (113 Å z-edge). The first three peaks, from left to right, are nitrogen (blue), central carbon (black), and methyl carbon (red). The zero of the x-axis corresponds to the position of the first oxygen layer.

can be seen, containing MeCN molecules that are typically antiparallel to the attached ones. In the classical simulation with the same cell, it can be seen that after 1 ns all sites are occupied with MeCN, forming an all-parallel monolayer with defects. In the DFT simulation the average distance of a titanium atom at the surface to the closest MeCN nitrogen is 2.42 Å; in the classical run this is 2.50 Å. The standard deviation of the average values is in both runs in the range 0.16–0.18 Å. A snapshot of the simulation is shown in figure 2. It can clearly be seen that the first solvent layer resembles closely the all-parallel monolayer configuration. All molecules in the first layer adopt well defined locations in the plane of the surface. However, two kinds of orientational defects can be observed: molecules in an antiparallel configuration and in an orthogonal orientation. From our MD simulations, we can infer that the lifetime of these defects is the 100 ps–1 ns range. From this snapshot, the second solvent layer can also be discerned. In this layer, there is a tendency to form antiparallel dimers with molecules from this and other layers. Such antiparallel dimers are also found in the high temperature (α) phase of solid acetonitrile [38]. The corrugation of the surface is visible in the first and second solvent layer.

To quantify these observations, we compute properties as a function of the distance to the surface, the z-position, in the following. Shown in figure 3 are the nitrogen density profiles as obtained with DFT and FF simulations. The DFT results, being averaged over only 5 ps, exhibit more statistical noise than the FF simulations. Nevertheless, there is good agreement between these simulations, in particular concerning the peak positions. The difference in the height of the first peak can be attributed to the fact that the equilibrium concentration of the orientational defects has not yet been reached in the DFT simulation, while in the much longer FF simulation this is the case. The very pronounced first peak indicates a tightly bound nitrogen atom, consistent with the calculations in the previous section. Further layers, extending at least 10 Å away from the surface, can be observed in the density profile, but in order to exclude sampling and size effects it is useful to focus on the FF results obtained for the larger system, shown in figure 4. In this figure, several more peaks can be seen, at least up to 20 Å away from the surface. The orientational defects seen in the first layer are the explanation for the appearance of an early second peak in the nitrogen profile at around 4.6 Å, and the double peak (2.2 and 3.5 Å) for the central carbon. The alternating orientation of the solvent molecules can be most clearly illustrated with a figure showing the distribution of the cosines of the angle between the MeCN axis and the surface normal with respect to the distance between the surface and the center of mass of these molecules. Indeed, figure 5 displays at least nine layers (17 Å) with alternating orientations, and

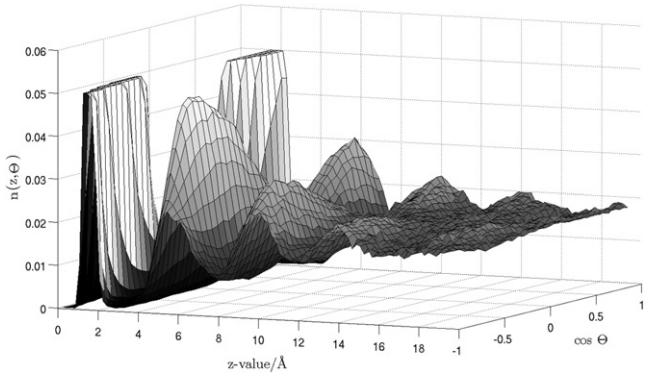

Figure 5. The distribution of the cosine of the angle between the surface normal and the MeCN dipole is shown with respect to the distance between the center of mass of the molecule and the surface. The alternating orientation of the successive solvent layer can clearly be seen.

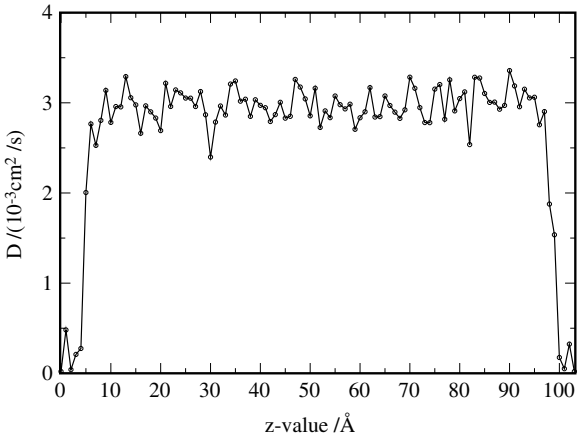

Figure 6. Shown is the self-diffusion constant of MeCN for diffusion parallel to the surface. The strongly suppressed diffusion near the interface can clearly be seen, despite the statistical noise due to the procedure used for computing the distance dependent diffusion constant (see the text for details).

underlines the tendency of MeCN to pair its dipole. Note that each peak in the density profile corresponds to approximately two peaks in the orientational profile, suggesting that the upper and lower parts of a layer (as defined by the density) have opposite orientations. The structure shown in figures 3 and 5 clearly suggests that the solvent properties near the interface will be significantly different from the properties in the bulk.

The last property we investigate in this section is the molecular dipoles of the solvent molecules, since it can be expected that the TiO_2 surface will have a strongly polarizing effect on close by MeCN molecules. This property cannot be obtained from a simple point charge FF model, but can be obtained from the DFT simulations using maximally localized Wannier functions [39, 40]. We have evaluated the molecular dipoles every 12.5 fs during the *ab initio* molecular dynamics simulation. We find a significant increase of the dipole from about 5.0 D in the liquid to approximately 6.3 D for those molecules directly interacting with the surface. However, the shift in the average dipole is already much reduced (5.2 D) in the second layer. The strongly enhanced dipole of the molecules in the first layer can in part explain the difficulty experienced by the FF in reproducing exactly the detailed energetics of the interactions as shown in table 2. We note, however, that a partial charge transfer from the nitrogen atom to the titanium atom, i.e. from the solvent to the solid, would appear in this analysis as an enhanced molecular dipole. Furthermore, such a charge transfer might be artificially large due to the self-interaction error present in local approximations to density functional theory. The distance dependent distributions of the molecular dipoles (not shown) indicate that the fluctuations of the dipoles around the average value are up to five times larger in the first two layers than in the bulk.

5. Solvent dynamics near the interface

In this section, the influence of the TiO_2 surface on the self-diffusion of MeCN will investigated, and the diffusion constant as a function of the distance with respect to the surface will be computed. These calculations are based on the approach of Liu *et al* [41] for calculating anisotropic diffusion constants near an interface. The central idea is to calculate the mean square displacements for those molecules i staying in the layer $[a, b]$ during the entire period $[t, t + \tau]$:

$$\langle \Delta x^2(\tau)\rangle_{[a,b]} = \frac{1}{T}\sum_{t=1}^{T}\frac{1}{N(t,t)}\sum_{i\in[a,b]_{[t,t+\tau]}}(x_i(t+\tau)-x_i(t))^2. \tag{1}$$

This function is then weighted by the probability for an particle to stay for time τ in this layer:

$$P(\tau) = \frac{1}{T}\sum_{t=1}^{T}\frac{N(t,t+\tau)}{N(t,t)}, \tag{2}$$

where $N(t, t+\tau)$ denotes the number of particles that remained in the interval $[a, b]$ during the entire period $[t, t + \tau]$, so that the self-diffusion constant for a given layer can be calculated as

$$D_{xx}([a,b]) = \lim_{t\to\infty}\frac{\langle \Delta x^2(\tau)\rangle_{[a,b]}}{2\tau P(\tau)}. \tag{3}$$

These formulas have been applied to the larger classical system; intervals $[a, b]$ of 1 Å lead to the best statistical accuracy. Nevertheless, as the function $P(\tau)$ decays relatively quickly to zero, only a short part of the mean square displacement curve can be employed to obtain an estimate of the diffusion constant, and some statistical uncertainty cannot be avoided. The results are shown in figure 6. Far away from the interface, the diffusion constant is fluctuating around 3×10^{-3} cm^2 s^{-1}. This in good agreement with the diffusion constant we have calculated for the bulk acetonitrile experimental density using the formula for diffusion in an isotropic liquid (2.93×10^{-3} cm^2 s^{-1}). This indicates that our simulation of the interface is properly equilibrated and at the correct pressure. Near the interface, at a distance of about 10 Å, the diffusion constant starts decreasing till it reaches a value close to zero in the first layer of MeCN. This behavior

can be explained by the molecular structure we have described in the previous section. Indeed, the relatively strong binding of the MeCN molecules to the TiO_2 surface immobilizes the first layer. The strong dipolar interactions between the subsequent layers of alternating orientation and the corrugation of the surface introduce a barrier for diffusion. We have observed that in these layers diffusion is a collective defect mechanism in which one molecule rotates out of the layer leaving a vacancy. This in turn allows for diffusion in the layer.

6. Discussion

Solids have traditionally been the domain of the plane wave community, while molecules have traditionally been studied with atom centered basis sets such as Gaussians. In this work, we have for the first time investigated a solid–liquid interface using the CP2K simulation package and the GPW approach. Our results indicate that this approach is well suited for both the molecular liquid and the slab, even though we find that the traditional split valence basis sets that dominate the molecular calculations are not well suited for calculations on solids. Our recently proposed molecularly optimized basis sets seem to perform well. The advantage of the GPW approach is that large systems, containing several hundreds of atoms, can be simulated efficiently, even allowing for Born–Oppenheimer molecular dynamics. Both capabilities are required for simulating solid/liquid interfaces, as such systems must be large and must be treated at a finite temperature, i.e. in the regime where the liquid exists as such. Nevertheless, despite the fact that a first DFT simulation of 1 ns has been performed using CP2K [42], long timescales (>1 ns) generally remain inaccessible to first principles molecular dynamics simulations. It is therefore required to employ computationally less demanding methods if these timescales must be probed. In this work, we have also used CP2K to perform FF based simulations of the interface. Not only is it convenient to be able to switch quickly between simulation methods, also the flexibility of the classical code, e.g. mixing potential types suited for various systems within one simulation, is advantageous for these systems. The force field has been derived and validated using first principles results, with satisfactory results for interaction energies and geometries. Nevertheless, we are aware of the limitations of a non-polarizable force field for the description of this system, and we have emphasized the strong polarization of molecules near the interface.

The interface we have studied, MeCN in contact with anatase(101), shows a rich structure. We find that the solvent interacts rather strongly with the solid, forming a well defined first solvent layer that might passivate the surface in DSSCs. The strong dipolar interactions between molecules and the fixed orientation of the molecules in the first layer introduce a pronounced layering of the solvent near the interface, with a tendency to form layers of alternating orientation. This structure extends, depending on the criterion used, up to 10–20 Å away from the interface. For DSSCs this is the region which contains the dye, and where light induced electron transfer and the dye re-reduction take place. From the FF simulations, we find a much reduced diffusion in the interfacial layer, which could imply that mass transport in the narrow channels of the mesoporous TiO_2 could be lower than anticipated. Furthermore, since the solvent structure near the interface differs significantly from the bulk structure, we expect solvent properties, e.g. the ability to solvate ions or the solvent dielectric constant to be different for the interface region and the bulk liquid. As these properties are central quantities in Marcus's theory of electron transfer, we are currently quantifying these effects with the force fields derived in this work. We believe that a further understanding of the interface induced changes of these properties might help to explain in part the observed differences between dyes in bulk solution and at the interface.

Acknowledgment

We would like to acknowledge the referee for insightful questions and for pointing out [38]. This work has been supported by the Swiss national science foundation under grant number 200020-111895.

References

[1] O'Regan B and Grätzel M 1991 *Nature* **353** 737
[2] Grätzel M 2001 *Nature* **414** 338
[3] Grätzel M 2003 *J. Photochem. Photobiol.* C **4** 145
[4] Tributsch H 2004 *Coord. Chem. Rev.* **248** 1511
[5] Duncan W R and Prezhdo O V 2007 *Annu. Rev. Phys. Chem.* **58** 143
[6] Fantacci S, De Angelis F and Selloni A 2003 *J. Am. Chem. Soc.* **125** 4381
[7] Pourtois G, Beljonne D, Moucheron C, Schumm S, Kirsch-De Mesmaeker A, Lazzaroni R and Bredas J L 2004 *J. Am. Chem. Soc.* **126** 683
[8] Perrson P and Lundqvist M J 2005 *J. Phys. Chem.* B **109** 11918
[9] Nazeeruddin M K, De Angelis F, Fantacci S, Selloni A, Viscardi G, Liska P, Ito S, Takeru B and Gratzel M G 2005 *J. Am. Chem. Soc.* **127** 16835
[10] Lundqvist M J, Nilsing M, Lunell S, Akermark B and Persson P 2006 *J. Phys. Chem.* B **110** 20513
[11] Onozawa-Komatsuzaki N, Kitao O, Yanagida M, Himeda Y, Sugihara H and Kasuga K 2006 *New J. Chem.* **30** 689
[12] Patthey L, Rensmo H, Persson P, Westermark K, Vayssieres L, Stashans A, Petersson A, Bruhwiler P A, Siegbahn H, Lunell S and Martensson N 1999 *J. Chem. Phys.* **110** 5913
[13] Stier W and Prezhdo O V 2002 *J. Phys. Chem.* B **106** 8047
[14] Rego L G C and Batista V S 2003 *J. Am. Chem. Soc.* **125** 7989
[15] Bandura A V and Kubicki J D 2003 *J. Phys. Chem.* B **107** 11072
[16] Marcus R A 1956 *J. Chem. Phys.* **24** 966
[17] Marcus R A and Sutin N 1985 *Biochim. Biophys. Acta* **811** 265
[18] Marcus R A 1993 *Rev. Mod. Phys.* **65** 599
[19] VandeVondele J, Lynden-Bell R, Meijer E J and Sprik M 2006 *J. Phys. Chem.* B **110** 3614
[20] VandeVondele J, Sulpizi M and Sprik M 2006 *Angew. Chem. Int. Edn* **45** 1936
[21] VandeVondele J, Sulpizi M and Sprik M 2007 *Chimia* **61** 155
[22] Sulpizi M, Raugei S, VandeVondele J, Carloni P and Sprik M 2007 *J. Phys. Chem.* B **111** 3969
[23] Izvekov S and Voth G A 2001 *J. Chem. Phys.* **115** 7196
[24] Izvekov S, Mazzolo A, VanOpdorp K and Voth G A 2001 *J. Chem. Phys.* **114** 3248
[25] Vassilev P, van Santen R A and Koper M T M 2005 *J. Chem. Phys.* **122** 054701

[26] CP2K version 2.0.0 (development version), the CP2K developers group 2007 freely available at http://cp2k.berlios.de/
[27] VandeVondele J, Krack M, Mohamed F, Parrinello M, Chassaing T and Hutter J 2005 *Comput. Phys. Commun.* **167** 103
[28] Lippert G, Hutter J and Parrinello M 1999 *Theor. Chem. Acc.* **103** 124
[29] VandeVondele J and Hutter J 2003 *J. Chem. Phys.* **118** 4365
[30] Perdew J P, Burke K and Ernzerhof M 1996 *Phys. Rev. Lett.* **77** 3865
[31] Goedecker S, Teter M and Hutter J 1996 *Phys. Rev.* B **54** 1703
[32] Hartwigsen C, Goedecker S and Hutter J 1998 *Phys. Rev.* B **58** 3641
[33] Krack M 2005 *Theor. Chem. Acc.* **114** 145
[34] VandeVondele J and Hutter J 2007 *J. Chem. Phys.* **127** 114105
[35] Lazzeri M, Vittadini A and Selloni A 1996 *Phys. Rev.* B **63** 155409
[36] Hutter J *et al* 2007 *CPMD (Car–Parrinello Molecular Dynamics): An Ab Initio Electronic Structure and Molecular Dynamics Program (IBM Zurich Research Laboratory (1990–2007) and Max-Planck-Institut für Festkörperforschung Stuttgart (1997–2001))* see http://www.cpmd.org/
[37] Grabuleda X, Jaime C and Kollman P A 2000 *J. Comput. Chem.* **21** 901
[38] Enjalbert R and Galy J 2002 *Acta Crystallogr.* B **58** 1005
[39] Marzari N and Vanderbilt D 1997 *Phys. Rev.* B **56** 12847
[40] Silvestrelli P L and Parrinello M 1999 *Phys. Rev. Lett.* **82** 3308
[41] Liu P, Harder E and Berne B J 2004 *J. Phys. Chem.* B **108** 6595
[42] Kühne T D, Krack M, Mohamed F R and Parrinello M 2007 *Phys. Rev. Lett.* **98** 066401